https://doi.org/10.5194/essd-2026-77
Preprint. Discussion started: 27 March 2026
© Author(s) 2026. CC BY 4.0 License.

Open Access Earth System Science Data Discussions

CAMS-REG-UNC-v8.1: A detailed uncertainty product for the gridded CAMS-REG-v8.1 emission inventory

Ingrid Super[1], David Mathas[1,2], Bastiaan Jonkheid[1,3], Arjo Segers[1], Jeroen Kuenen[1]

[1]Department of Air Quality and Emissions Research, TNO, P.O. Box 80015, 3508 TA Utrecht, the Netherlands
[2]Earth Sciences Department, Barcelona Supercomputing Center, Plaça Eusebi Güell, 1-3 08034 Barcelona, Spain
[3]Department of Geodata and Information Management, TNO, P.O. Box 80015, 3508 TA Utrecht, the Netherlands

Correspondence to: Ingrid Super (ingrid.super@tno.nl)

Abstract. Independent verification of greenhouse gas emission reductions and trends in air pollution levels is receiving increasing attention. Atmospheric observations can provide such a constraint on emission estimates through inverse modelling, which requires a detailed quantification of uncertainties in prior emission inventories, observations and chemical transport models. This paper describes a detailed methodology to quantify uncertainties in a state-of-the-art European emission inventory: CAMS-REG. Uncertainties are estimated for all input data used to create the emission inventory and propagated to the final product. This results in separate uncertainty estimates for country-level emissions per sector and uncertainties in the spatial allocation of those emissions. Ideally, the gridded emission uncertainties should add up to the country-level emission uncertainties and for this purpose an optimization procedure was developed (only for countries with detailed emission reporting). This results in (scaled) gridded emission uncertainties and spatial error correlation lengths, which are included in the final dataset. The gridded uncertainty maps show large differences between pollutants and countries, representing the variability in input data and their reliability. CO_2 shows the smallest gridded (optimized) uncertainties, with a median relative standard deviation of 15 % (interquartile range: 9 % – 25 %). The largest gridded (optimized) uncertainties are found for NMVOC: 45 % (38 % – 58 %). This work follows up from previous efforts and details the first comprehensive emission uncertainty dataset for Europe. The data are available from Zenodo: https://doi.org/10.5281/zenodo.18400810 (Super et al., 2026).

1 Introduction

Effective climate change mitigation and reducing the negative health impacts of air pollution asks for continuous accounting of greenhouse gas and air pollutant emissions. In Europe, most countries report total emissions of both greenhouse gases and air pollutants annually (EMEP, 2023; UNFCCC, 2024). These emissions are based on statistical data of activity rates and estimated emission factors, a so-called 'bottom-up' emission inventory. An emission inventory is an accounting system that details how much of a certain trace gas is being emitted to the atmosphere over a specific domain and time window. Emission inventories are widely used to support science and decision-making in the field of air pollution exposure and climate mitigation (e.g., Albarus et al., 2023; Scarpelli et al., 2024; Siouti et al., 2025; Tokaya et al., 2024).

https://doi.org/10.5194/essd-2026-77
Preprint. Discussion started: 27 March 2026
© Author(s) 2026. CC BY 4.0 License.

Open Access Earth System Science Data Discussions

The demand for independent verification of these emission inventories using atmospheric observations is increasing, e.g., in support of the Paris Agreement (European Commission, 2018), to improve national inventories, and to inform national reduction targets (German et al., 2021). Also in the field of air pollution, modelled atmospheric concentrations of air pollutants can be compared to observations for validation purposes and to inform scientists about the accuracy of the emission inventories and atmospheric transport models (e.g., Musollari et al., 2025; Tokaya et al., 2024; Van der A et al., 2024; Wang et al., 2024). When atmospheric observations are used to constrain the input emission data, we refer to this as inverse modelling.

Inverse modelling is a statistical method to optimize a system based on its uncertainties. In the current context, the system consists of input parameters to be optimized (prior emissions), chemical transport models, and atmospheric observations. Here, prior emissions are spatially explicit, which are available at global (Crippa et al., 2018; Doumbia et al., 2021; McDuffie et al., 2020) and regional scales (Gurney et al. 2020; Keita et al. 2021; Kuenen et al., 2022; Kurokawa and Ohara 2020). In this remainder of this work, we reserve the term 'emission inventory' for spatially resolved emission datasets.

The aim of inverse modelling is to find the optimal solution that minimizes the uncertainties at the lowest cost (i.e., the best match between observed and modelled trace gas concentrations). The larger the uncertainty in one of the components, the less information can be gained from it, and the larger the freedom to move away from its starting point. Therefore, a good quantification of uncertainties in each of these components is essential to get reliable output. However, uncertainty quantification in emission inventories is a difficult topic. Often, scientists rely on sensitivity analyses (Lorente et al., 2019), intercomparison studies (Gately and Hutyra, 2017; Hutchins et al., 2017; Oda et al., 2019; Pillai et al., 2016), or expert judgement (Lauvaux et al., 2016; Tenkanen et al., 2024) to estimate the prior emission uncertainty. Error correlations are often neglected, although sometimes a spatial error correlation length is estimated based on expert judgement. A more elaborate study was done by Hogue et al. (2016) for the US, considering multiple sources of uncertainty. However, as far as we are aware, no gridded emission uncertainty data products are currently available.

This paper describes the methodology developed to quantify uncertainties in the widely-used CAMS-REG European emission inventory. The CAMS-REG emission inventory (Kuenen et al., 2022) is developed by the same researchers that contributed to this paper, which allows us to estimate the uncertainty in each of the input parameters and propagate those uncertainties to the final product. The emission uncertainties are fully consistent for all air pollutants and greenhouse gases in the inventory. Here, we illustrate the full dataset (CAMS-REG-UNC), which builds on previous work (Super et al., 2020; 2024) and now covers uncertainty estimates for all species included in the inventory. A major improvement compared to previous publications is the development of an optimization procedure that ensures consistency between country-level, reported emission uncertainties and the gridded uncertainties through the use of a spatial error correlation length. This allows users to use the dataset at multiple scales and aggregation levels.

https://doi.org/10.5194/essd-2026-77
Preprint. Discussion started: 27 March 2026
© Author(s) 2026. CC BY 4.0 License.

Open Access Earth System Science Data Discussions

2 Methods

Estimating uncertainties in data products can be done in different ways. Here, we choose to define uncertainties at the most detailed level possible and propagate those uncertainties to the final product (Figure 1). This work is done by the same group of researchers responsible for processing the emissions data, which allows us to take stock of the detailed knowledge of the input parameters and assumptions that are made during the preparation of the CAMS-REG inventory.

In the following sub-sections, we describe the emission inventory, the sources of uncertainty, the data used to estimate those uncertainties, and the processing steps to get to the final product. The processing steps are different for countries with detailed emission reporting (Annex-I countries), other countries (mostly North Africa and Middle East), and sea regions (see Table A1 for a list of regions and to which category they belong). Note that some of these methods have been described previously (Super et al., 2024), but several changes and improvements have been made.

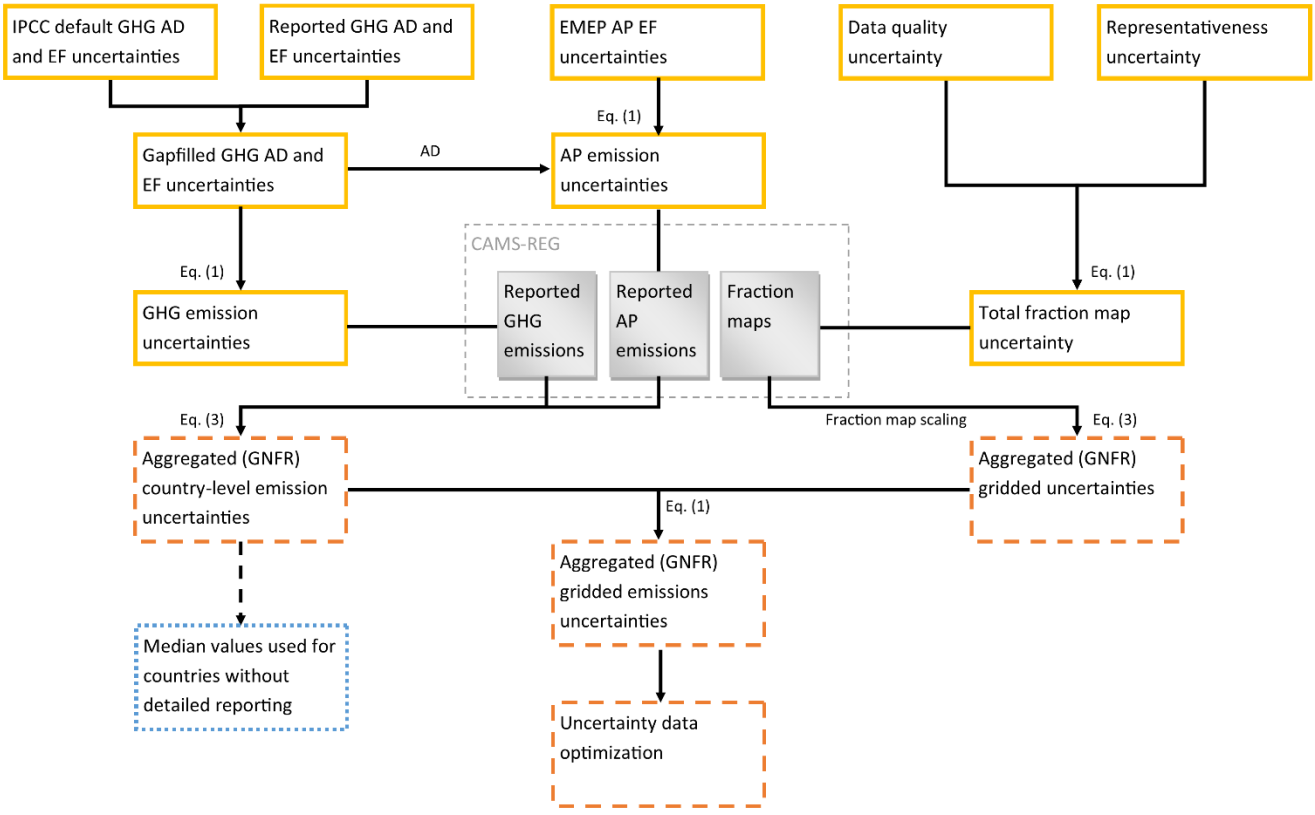

Figure 1: Flow diagram showing the error propagation process for countries with detailed emission reporting. Yellow, solid boxes are related to the uncertainty input and orange, dashed boxes to the aggregated (GNFR: Gridded Nomenclature For Reporting) uncertainty output. The blue dotted box indicates where the emission uncertainties for countries without detailed emission reporting come from. GHG and AP refer to greenhouse gases and air pollutants, respectively. AD and EF refer to activity data and emission factors, respectively.

https://doi.org/10.5194/essd-2026-77
Preprint. Discussion started: 27 March 2026
© Author(s) 2026. CC BY 4.0 License.

Open Access Earth System Science Data Discussions

2.1 European emission inventory

The emission inventory used as a basis for this work is the CAMS-REG v8.1 for 2022, described in detail by Kuenen et al. (2022). This emission dataset is the state-of-the-art gridded emission inventory for Europe with a spatial resolution of 0.1 ° by 0.05 °. It contains emissions of greenhouse gases (CO_2, CH_4) and air pollutants (CO, NO_x, PM2.5, PM10, NMVOC, NH_3, SO_x) per GNFR (Gridded Nomenclature For Reporting) sector, with an additional split for road transport, as indicated in Table 1.

Table 1: Overview of GNFR sectors and the 95 % confidence interval (in %) of CO_2 and CH_4 emissions for countries without detailed emission reporting. These intervals are based on the median GNFR-level uncertainties for countries with detailed emission reporting (see Sect. 2.2.1). NA = Not applicable.

GNFR sector	CO_2	CH_4
A – Public power	3	47
B – Industry	2	25
C – Other stationary combustion	4	52
D – Fugitives	11	39
E – Solvents	19	39
F1 – Road transport – gasoline	2	21
F2 – Road transport – diesel	2	18
F3 – Road transport – LPG	2	22
F4 – Road transport – non-exhaust	NA	NA
G – Shipping	6	55
H – Aviation	7	81
I – Off-road transport	5	40
J – Waste	34	30
K – Agriculture livestock	NA	19
L – Agriculture other	43	55

The CAMS-REG emission inventory is based as much as possible on emission reports from individual countries. For greenhouse gases, Annex-I countries report their emissions on an annual basis to the UNFCCC (UNFCCC, 2024) and for air pollutants emission reports are delivered to the EMEP (European Monitoring and Evaluation Programme) Centre on Emission Inventories and Projections (EMEP, 2023). These reports contain country-level emissions for over 250 detailed sector/fuel combinations, which are spatially distributed using a wide range of fraction maps. Fraction maps describe the share of the country-level emissions occurring within each grid cell based on spatial proxy data (e.g., population density or land use), and therefore their sum is always one for a country. Finally, the gridded emissions are aggregated to the GNFR sectors.

https://doi.org/10.5194/essd-2026-77
Preprint. Discussion started: 27 March 2026
© Author(s) 2026. CC BY 4.0 License.

Most shipping activities are of international nature, taking care of transport between countries, and are therefore not included in national total emissions. Some countries report (part of) the international shipping emissions, but these provide an incomplete picture of shipping emissions in Europe. Therefore, CAMS-REG uses the shipping emissions from the STEAM model (Jalkanen et al., 2012; Johansson et al., 2017), that provides gridded emissions on the CAMS-REG grid definition. The emissions are based on AIS (Automatic Identification System) data and vessel characteristics and cover all pollutants in the CAMS-REG dataset. Additionally, for countries without detailed emission reporting, where emission reporting is incomplete, or the quality of the reporting is poor, other datasets are used to estimate emissions per GNFR sector.

2.2 Emission uncertainty estimates

The main source of uncertainty in the emission inventory is related to the input data used for the CAMS-REG inventory (see also Figure 1). The reported annual, country-level emissions have an uncertainty, which is determined largely by the applied methodology and the quality of the data used for those calculations. For example, countries can decide to use a default method or emission factor, or a country-specific approach. Generally, the first option results in a higher uncertainty. Additionally, we identify two sources of uncertainty in the spatial disaggregation. First, the quality of the proxy data itself is a source of uncertainty. For numerical data, the data quality indicates the accuracy of the values provided. For categorial variables, this often translates into a correct categorization of each grid cell, for example whether a grid cell identified as grassland is indeed grassland. Second, an important source of uncertainty is the representativeness of a proxy, i.e., how well does a proxy represent the actual location and magnitude of activities that cause emissions.

The data used to estimate these uncertainties are detailed in the next sub-section. Other sources of uncertainty are, for example, the discrete nature of the grid and possible double-counting or missing sources (systematic errors). We do not consider these sources of uncertainty.

2.2.1 Country-level emission uncertainties

Most Annex-I countries that report their greenhouse gas emissions also include an uncertainty estimate, although this is not mandatory. This uncertainty estimate can be more or less detailed in terms of sector (dis)aggregation, but at least provides an uncertainty for activity data (AD) and emission factors (EF) separately and often differentiates between fuel types.

First, we collected the reported uncertainties from 29 countries for the reporting year 2020 (UNFCCC, 2024). Generally, the reported uncertainties vary little from one reporting year to the next, except for some typos or when the methodology for the emission calculations has changed. A few typos identified for Italy were corrected based on a discussion with the reporting agency. Although more typos may occur, we are unable to identify those without detailed knowledge of the methodologies applied by each country and a discussion with the reporting agencies, which would be impossible to achieve. Therefore, we assume the reported uncertainties to be valid for the year considered. Estonia provided multiple uncertainty estimates for several sectors, separating between different activities within a sector, and we made an assumption about the most dominant activity. This didn't occur for other countries.

https://doi.org/10.5194/essd-2026-77
Preprint. Discussion started: 27 March 2026
© Author(s) 2026. CC BY 4.0 License.

Second, gap filling is applied to cover all sector/fuel combinations and countries. If a country reports uncertainties at a more aggregated sector level, we assume this uncertainty to be representative for the more detailed sub-sectors, but only up to a certain level. For example, uncertainties for road transport can be used for all vehicle types, but a more aggregated uncertainty (e.g., for mobile sources as a whole) is assumed to be unreliable. Next, for each sector/fuel combination, we take the uncertainties from all countries that report an uncertainty, and calculate the median value. This median value is then applied to all countries without uncertainty information for that particular sector/fuel combination after applying the first gap filling step. In very few cases uncertainty information is lacking completely for a specific sector/fuel combination and IPCC default values are used (Eggleston et al., 2006).

Air pollutant emission uncertainties are generally not reported by the countries. However, in most cases, the AD is shared between the greenhouse gases and air pollutants and the reported greenhouse gas AD uncertainty is used consistently for all trace gases. The EMEP/EEA Guidebook provides a global Tier-1 uncertainty estimate for the air pollutant EFs (European Environment Agency, 2019), which is applied to all countries. Additionally, a generic uncertainty range is applied to sector/fuel combinations without an uncertainty estimate, as listed in Chapter 5 of the EMEP/EEA Guidebook. The range is chosen based on expert judgement of the quality of the EF estimate.

The greenhouse gas and air pollutant emission uncertainties are propagated to the GNFR level (explained in Sect. 2.3). The median GNFR-level emission uncertainties are applied to countries without detailed emission reports (Table 1, Figure 1).

International shipping falls under the same GNFR category as inland shipping, but it is treated separately, as the emissions are not reported by countries. The AD uncertainty estimate for international shipping is based on a comparison of the STEAM model predictions with fuel reporting (J.-P. Jalkanen, personal communication, August 25, 2022). Emission factors uncertainties are estimated by Grigoriadis et al. (2021).

A table with country-level emission uncertainty ranges per sector/fuel combination is provided as supplementary material.

2.2.2 Proxy data uncertainties

The proxies used for the spatial disaggregation of country-level emissions are mostly based on open-source datasets. Therefore, the data quality is taken from metadata or publications from the data providers where possible. In some cases, the uncertainty estimate of other, similar datasets is used. Where such information is not available expert judgement was needed. The uncertainty values are summarized in Table 2, including the source of these estimates.

It is important to note that if grid cells falsely contains no data (zero value or the wrong category) this cannot be solved in an inversion system by including an uncertainty estimate (scaling a value of zero remains zero). This also affects point source locations. We have seen examples where the coordinates of an industrial facility were actually pointing to the headquarters of the company, which could be at a completely different location than where the emitting activity takes place. Therefore, a lot of resources have been invested in placing large point sources at their correct location and we assume the spatial allocation of point sources has no uncertainty.

https://doi.org/10.5194/essd-2026-77
Preprint. Discussion started: 27 March 2026
© Author(s) 2026. CC BY 4.0 License.

Open Access Earth System Science Data Discussions

Table 2: Overview of proxy data (in general terms) and the uncertainties (95 % confidence interval) related to the quality of the data and the representativeness. For the data quality references are listed where possible and for the representativeness error a justification is provided.

Proxy data	Data quality uncertainty (%)	Reference	Representation uncertainty (%)	Justification
Land use	0	Thematic accuracy is >85 % at high resolution (Copernicus, 2024); at our resolution the error is negligible.	200	Land use classification is poorly representative of the activities taking place on those land uses.
Population	18	Archila Bustos et al. (2020)	10-200	For residential emissions the representation is good, for commercial sectors a little less and as a default proxy very poor.
Residential wood combustion	50	Expert judgement; Grythe et al. (2019)	50	Expert judgement.
Gas distribution	18	Largely based on population.	40	Expert judgement.
Road transport	15	Estimated uncertainties in traffic models (Gao et al., 2010; Raney et al., 2003), reduced by the coarse resolution of our data.	10	The representation is assumed to be good, as emissions only occur on the road network.
Railways	200	Expert judgement.	0	Expert judgement.
Inland waterways	60	Expert judgement.	10	The representation is assumed to be good, as emissions only occur on the main waterways.
Livestock numbers	84-200	Robinson et al. (2014)	10	Livestock numbers are assumed to be representative for livestock-related emissions.
Fertilizer/ manure application	15	Expert judgement.	10	Expert judgement.
Agricultural waste burning	60	Andela et al. (2013)	10	Expert judgement.

https://doi.org/10.5194/essd-2026-77
Preprint. Discussion started: 27 March 2026
© Author(s) 2026. CC BY 4.0 License.

Open Access Earth System Science Data Discussions

The locations of most sources are relatively well-known, but the actual activity rate at any given location may be more difficult to assess through spatial datasets. For example, the road network is well-known, but traffic intensity may vary strongly between road segments. Similarly, population may be a reasonable proxy for residential combustion emissions, but in more densely populated areas the fuel consumption per household is often lower than in rural areas. Therefore, we add a representativeness error for each proxy, which is based on expert judgement (see Table 2 for a justification). Whereas the data quality is always the same for a proxy, the representativeness error depends on the sector it is applied to. For example, population is sometimes used as a default proxy and in that case the error is larger than when it is used for residential combustion.

The representativeness error increases the uncertainty per grid cell, but it also causes errors to be spatially correlated between grid cells that are nearby and have similar characteristics. This is expressed through a spatial correlation length, which will be explained in more detail in Sect. 2.4.

For countries without emission reporting we take spatially explicit emissions directly from other datasets and the proxy maps are not applied. As we lack information on the reliability of the spatial patterns in those datasets, we set the spatial uncertainty to 200 % (95 % confidence interval) for all GNFR sectors. For international shipping we set the spatial uncertainty to 60 % (95 % confidence interval), based on the accuracy and coverage of the AIS data and additional uncertainties in the STEAM model.

2.3 Error propagation

For countries with detailed emission and uncertainty data, the emissions are a product of the AD and EF. Therefore, the AD and EF uncertainties can be used to estimate uncertainties in emissions E:

$$\frac{\sigma_E}{E} = \sqrt{\left(\frac{\sigma_{AD}}{AD}\right)^2 + \left(\frac{\sigma_{EF}}{EF}\right)^2} \quad (1)$$

Here, σ is the standard deviation and the standard deviation divided by the parameter value denotes a relative uncertainty. The reported uncertainties are provided as a normalized 95 % confidence interval, so no knowledge on the values of AD and EF are needed. However, the uncertainty ranges are often lognormal. Since Eq. (1) assumes Gaussian errors, we calculate the Gaussian relative standard deviation from the confidence interval:

$$\frac{\sigma_X}{X} = \frac{(\ln(lim_{upper}) - \ln(lim_{lower}))}{4} \quad (2)$$

Here, lim_{upper} and lim_{lower} are the upper and lower limit of the 95 % confidence interval of variable X, respectively.

The emission uncertainties per sector/fuel combination (*sub*) are aggregated to the GNFR sector (*agg*):

$$\sigma_{E,agg} = \sqrt{\sum_{i=s}^{n} \sigma_{E,sub,s}^2} \quad (3)$$

Note that we use absolute standard deviations here, so we need to multiply the output from Eq. (1) with the emission values.

The two sources of uncertainty in the spatial disaggregation are combined following Eq. (1), where AD and EF are replaced by the data quality and representativeness error estimates (Table 2). Next, the spatial uncertainties are aggregated to the GNFR

https://doi.org/10.5194/essd-2026-77
Preprint. Discussion started: 27 March 2026
© Author(s) 2026. CC BY 4.0 License.

sector following Eq. (3), where the uncertainties per sector/fuel combination are replaced by the uncertainties per proxy. However, we cannot directly use the gridded fractions to calculate the absolute standard deviations, as the sum of all fractions per country and sector needs to be equal to one for an aggregated sector. Therefore, we scale each fraction map based on its relative contribution to the GNFR sector emissions per trace gas and country. These scaled fractions are then used to calculate the absolute standard deviations used in Eq. (3). Note that, even though the uncertainty per proxy is the same all over the grid, the final gridded uncertainties per GNFR sector vary per grid cell due to the different contributions of each proxy in a grid cell.

Finally, we add the uncertainties in country-level emissions to the uncertainties in the grid cells belonging to that country (using Eq. (1), where AD and EF are replaced by the country-level emission and gridded uncertainty), per GNFR sector and trace gas. With this, we cover uncertainties in the emissions and the spatial distribution.

For sea shipping, first Eq. (1) is applied to calculate the emission uncertainty per sea region, and then this value is combined with the spatial uncertainty. For countries without detailed emission reporting, only this final step is applied, as all input parameters are already specified at the GNFR emission level. In both cases, the gridded uncertainty shows no spatial variability.

2.4 Uncertainty data optimization

The results from the previous steps provide gridded emission uncertainties based on uncertainties in the input data. If we think of the gridded emission uncertainties within a country as diagonal elements in a covariance matrix ($\sigma(X_i)$, where X_i represents one element from n gridded uncertainties), the sum of all elements is the total country-level uncertainty, assuming no error correlations exist:

$$\sigma_{sum} = \sqrt{\sum_i^n \sigma(X_i)^2} \quad (4)$$

However, the sum of the elements (σ_{sum}) is not equal to the reported country-level uncertainties ($\sigma_{country}$), as the uncertainties in the proxies are independent from the country-level data. Therefore, we developed an optimization procedure, which matches the sum of all gridded uncertainties to the country-level uncertainties. The reason for setting the country-level uncertainties as our benchmark is that these are well-documented and consistent across the domain.

For the optimization, we introduce a spatial error correlation length, which is defined as the maximum distance over which the error in two grid cells is correlated, following an exponential decay with distance:

$$r_{i,j} = e^{-d_{i,j}/L} \quad \text{for } L >= 0 \quad (5)$$

Here, r is the (positive) correlation coefficient between location i and j, d is the distance between location i and j, and L is the spatial correlation length, following Kunik et al. (2019). As mentioned before, it is fair to assume spatial error correlations exist related to the representativeness error in the fraction maps.

Whereas uncorrelated errors tend to cancel each other out, positively correlated errors add up to larger total uncertainties. Therefore, we can use the spatial error correlation length to match the gridded uncertainties to the country-level uncertainty by introducing a covariance in Eq. (4):

https://doi.org/10.5194/essd-2026-77
Preprint. Discussion started: 27 March 2026
© Author(s) 2026. CC BY 4.0 License.

Open Access Earth System Science Data Discussions

$$\sigma_{sum} = \sqrt{\sum_i^n \sigma(X_i)^2 + \sum_i \sum_{j \neq i} Cov(X_i, X_j)} \quad (6)$$

Here, $Cov(X_i, X_j)$ is the covariance between elements X_i and X_j from n gridded uncertainties, which is a function of the uncertainties in X_i and X_j and their error correlation.

There are two options to solve Eq. (6). Option one is to choose a spatial error correlation length such that the sum of the variances and covariances equals the country-total uncertainty, but this can result in unrealistic values for the correlation length. Option two is to pick a reasonable correlation length and scale the gridded uncertainties. However, we wish to maintain the physical properties of the emission inventory, such that the uncertainties are physically meaningful as well. Therefore, we choose an flexible approach, as depicted in Figure 2, which first tries to select an appropriate correlation length within certain bounds and, if this does not result in a good agreement, it scales the gridded uncertainties. Note that the optimization is done per country and we assume no error correlations exist between pollutants and sectors.

The first step in the process is to determine a distance matrix, which is done using the Spherical Law of Cosines (Kuipers, 1999; Van Brummelen, 2017). Based on this, we can formulate a correlation matrix, using Eq. (5). The minimum correlation length is set to 0 km and the maximum correlation length to half the maximum distance between two grid cells within the country. Next, we calculate the aggregated uncertainty (Eq. (6)) for both the minimum ($\sigma_{sum,min}$) and maximum ($\sigma_{sum,max}$) correlation length and compare the results against the reported country-level uncertainty. If $\sigma_{sum,min}$ exceeds $\sigma_{country}$ the gridded uncertainties are scaled down and L remains zero. If $\sigma_{country}$ exceeds $\sigma_{sum,max}$ the correlation length is set to its maximum value and the gridded uncertainties are scaled up. In all other cases, Brent's method (Press et al., 1992) (using Python's Scipy package) is used to find the optimal correlation length and no scaling is applied to the gridded uncertainties. The output of the optimization is a scaling factor for the gridded uncertainties and a spatial error correlation length per country, sector and pollutant.

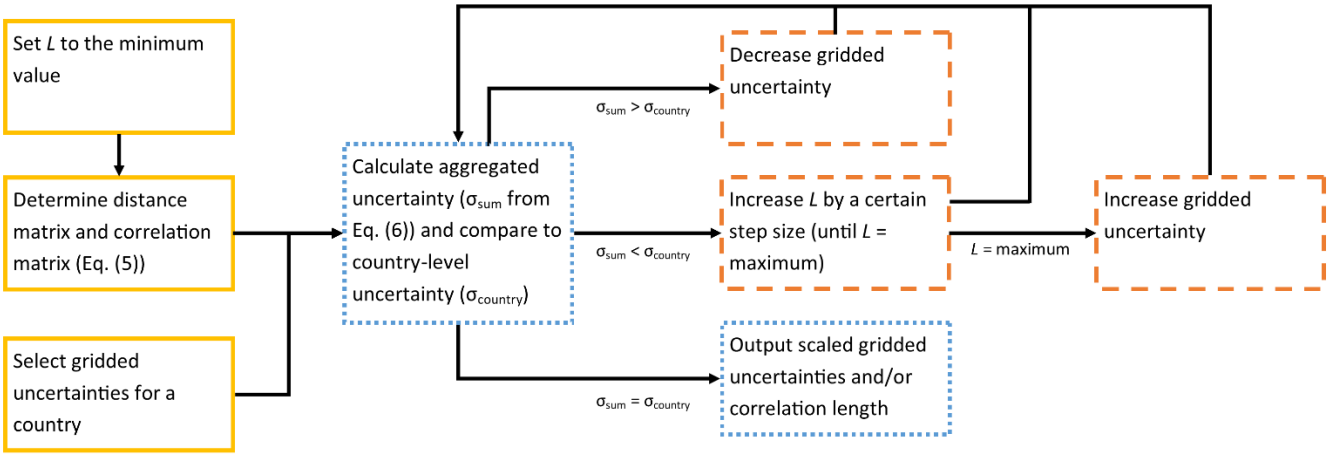

Figure 2: Flow diagram showing the optimization procedure for the gridded uncertainties. Yellow, solid boxes are related to the initialization and orange, dashed boxes to the optimization.

https://doi.org/10.5194/essd-2026-77
Preprint. Discussion started: 27 March 2026
© Author(s) 2026. CC BY 4.0 License.

Countries without detailed emission reporting and sea regions have no reliable region-total uncertainty and therefore the optimization is not applied to those regions. Russia is also excluded from the optimization, as it only falls partially within our domain and therefore the sum of the gridded uncertainties do not necessarily have to match the country-level uncertainties. Moreover, point sources are excluded from the optimization. As we assume no spatial uncertainty for point sources, no spatial error correlation exists between them and their uncertainty consists only of the emission uncertainty. We extract point source emissions and their uncertainty contribution from the country-total emissions and uncertainty before running the optimization. This means the spatial error correlation length should only be applied to the area sources.

3 Results

Most results are presented in box plots. In these plots, the boxes represent the interquartile range (IQR; Q1 to Q3), with the line indicating the median (Q2). The whiskers extend to maximum 1.5 times the IQR and outliers are not shown. All uncertainties are presented as relative standard deviation (σ), unless explicitly mentioned otherwise.

3.1 Country-level emission uncertainties

The country-level emission uncertainties form the basis of the final product, as they serve as direct input to the error propagation process and as a constraint in the optimization. Therefore, they have a significant impact on the final uncertainties. Figure 3 shows the spread in country-level emission uncertainties per pollutant, for which the sectoral uncertainties are aggregated per country. The CO_2 emission uncertainties are low (0.01 (median) (0.01 – 0.02 (IQR))), because the emission factors are well-known and stable. Moreover, CO_2 emissions are predominantly from combustion activities, for which activity data are easier to estimate than, for example, fugitive emissions. Additionally, the range in country-level emission uncertainties for CO_2 is small, because the reported uncertainties are very similar across countries.

https://doi.org/10.5194/essd-2026-77
Preprint. Discussion started: 27 March 2026
© Author(s) 2026. CC BY 4.0 License.

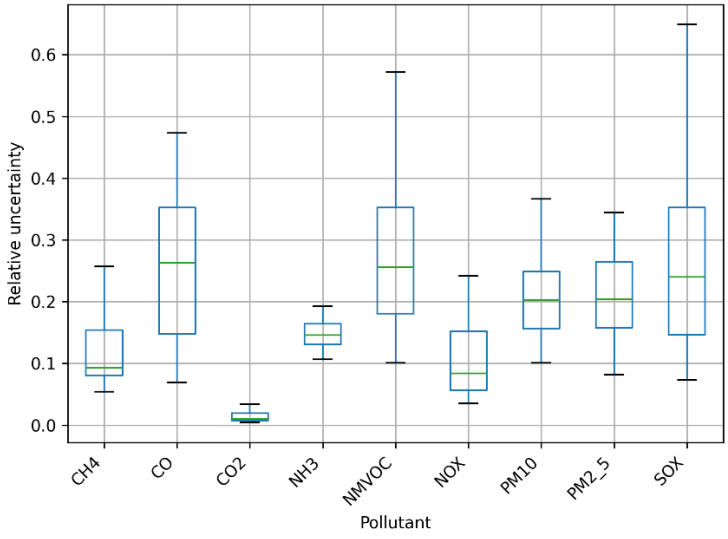

Figure 3: Box plot of total country-level emission uncertainties (summed over all sectors) per pollutant.

In contrast, the uncertainty ranges for SO_x (0.24 (0.15 – 0.35)), NMVOC (0.26 (0.18 – 0.35)) and CO (0.26 (0.15 – 0.35)) are large, which is related primarily to the significantly larger uncertainty in emission factors of the dominant emission sectors compared to CO_2. Figure 4 shows the spread in country-level CO emission uncertainties per sector. The other stationary combustion sector has a high emission uncertainty and can be a major source of CO emissions in a country. For example, in Estonia about 57 % of all CO emissions come from the other stationary combustion sector, which results in a country-total uncertainty of 39 %. In other countries, the contribution from this sector can be relatively small, for example, when the main fuel type is natural gas or limited heating is needed due to a warm climate. In Iraq, over 90 % of all CO emissions are attributed to road transport, which has a much lower uncertainty, and the country-total uncertainty adds up to 14 %. Hence, the country-level uncertainty depends on the sector contributions and the emission uncertainty associated with the dominant sectors.

The uncertainty ranges for CH_4, NH_3, NO_x, PM10, and PM2.5 are (0.09 (0.08 – 0.15)), (0.15 (0.13 – 0.16)), (0.08 (0.06 – 0.15)), (0.20 (0.16 – 0.25)), and (0.20 (0.16 – 0.26)), respectively.

https://doi.org/10.5194/essd-2026-77
Preprint. Discussion started: 27 March 2026
© Author(s) 2026. CC BY 4.0 License.

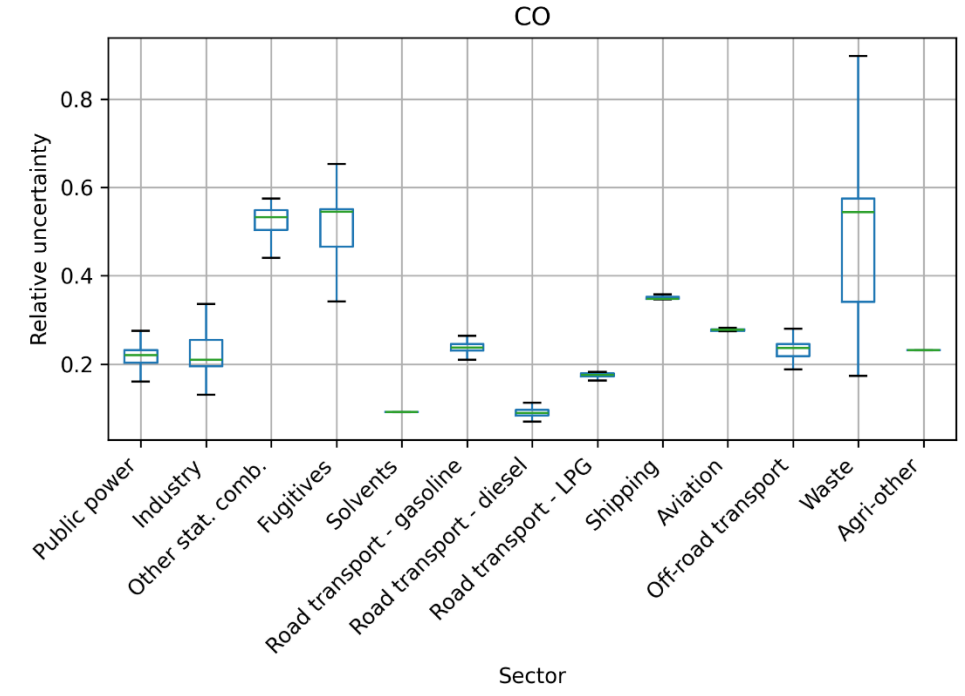

280 **Figure 4: Box plot of country-level CO emission uncertainties per sector.**

3.2 Gridded emission uncertainties

The final product consists of gridded uncertainties, which have been optimized for countries with detailed emission reporting (Sect. 2.4). The uncertainties are presented as a relative standard deviation, and can be translated into absolute standard deviations using the gridded emission values. Both relative and absolute gridded emission uncertainties for selected pollutants
285 are shown in Figure 5 (area sources only). A summary of the gridded uncertainties is provided in Table 3.

Table 3: Summary of median (IQR) relative uncertainties for countries with detailed emissions reporting and optimization (Optimized) and for countries without detailed emissions reporting and optimization (Non-optimized).

	Optimized	Non-optimized
CH_4	0.37 (0.34 – 0.41)	0.99 (0.81 – 1.00)
CO	0.42 (0.31 – 0.54)	0.80 (0.76 – 1.03)
CO_2	0.15 (0.09 – 0.25)	0.78 (0.68 – 1.02)
NH_3	0.36 (0.28 – 0.42)	0.88 (0.77 – 0.98)
NMVOC	0.45 (0.38 – 0.58)	0.94 (0.64 – 1.04)
NO_x	0.26 (0.12 – 0.40)	0.94 (0.81 – 1.08)
PM10	0.39 (0.32 – 0.47)	0.89 (0.70 – 0.97)
PM2.5	0.37 (0.32 – 0.42)	0.82 (0.70 – 0.92)

https://doi.org/10.5194/essd-2026-77
Preprint. Discussion started: 27 March 2026
© Author(s) 2026. CC BY 4.0 License.

SO_x	0.38 (0.29 – 0.44)	0.84 (0.70 – 1.02)

The absolute uncertainties follow largely the spatial patterns in emissions, with high absolute uncertainties in those places where high emissions occur. The maps of relative uncertainties show large jumps between countries, which is due to differences in the total country-level emission uncertainties. A country with a high overall uncertainty will, in general, receive larger gridded uncertainties. However, these patterns differ per pollutant. While CH_4 shows a relatively smooth relative uncertainty over Europe, CO and NH_3 show particularly large differences between countries. The sector mix will have a large impact on these patterns, as discussed before.

https://doi.org/10.5194/essd-2026-77
Preprint. Discussion started: 27 March 2026
© Author(s) 2026. CC BY 4.0 License.

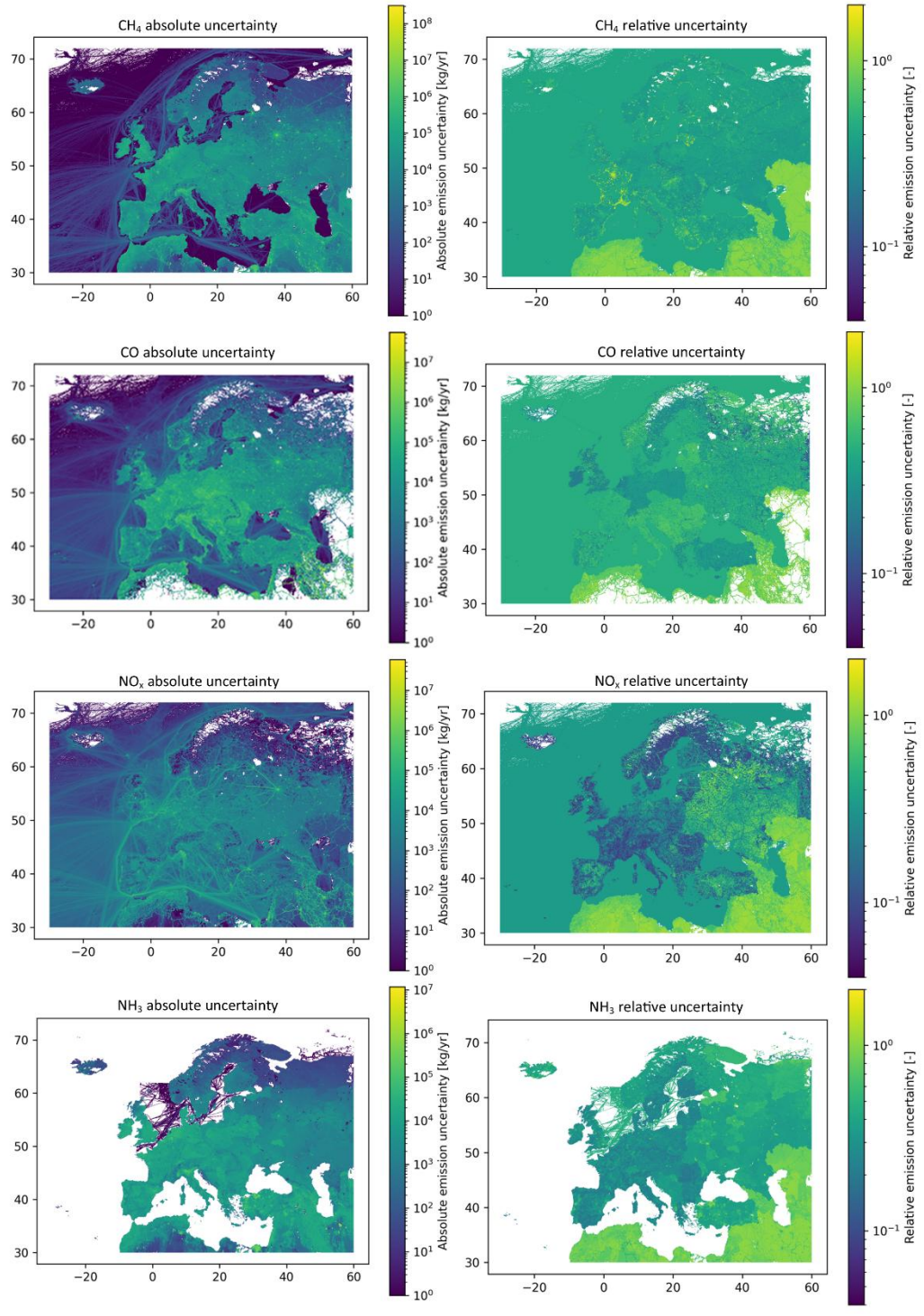

Figure 5: Maps of absolute and relative gridded emission uncertainties for selected pollutants. All colour scales are lognormal, where the same scale is applied for the relative uncertainties.

https://doi.org/10.5194/essd-2026-77
Preprint. Discussion started: 27 March 2026
© Author(s) 2026. CC BY 4.0 License.

3.3 Optimization parameters

The final product contains spatial error correlation lengths, following from the optimization procedure. These correlation lengths are defined for each specific country/sector/pollutant combination and should be applied to the area sources only (point sources have no correlation length). Note that correlation lengths are only available for countries for which the optimization procedure was performed (N = 41).

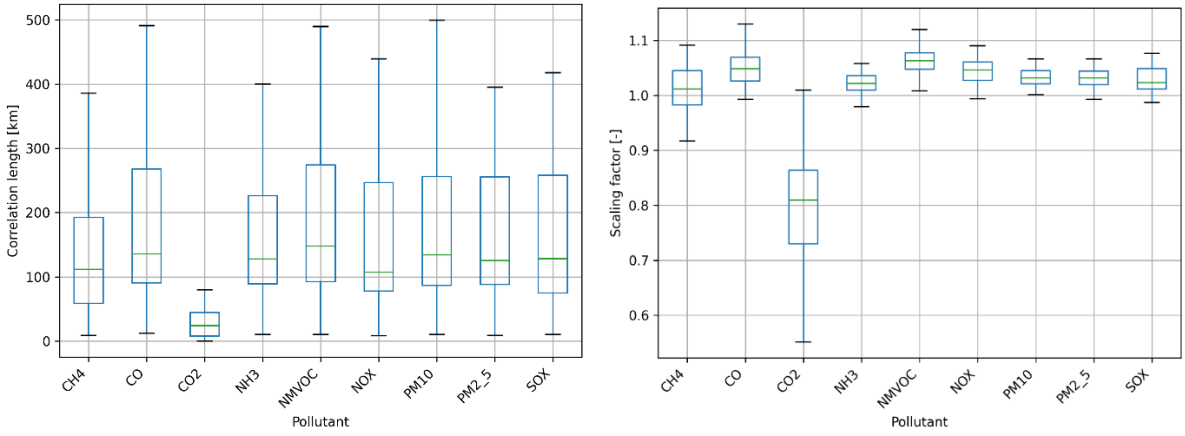

Figure 6: Box plot of country-specific correlation lengths (left) and scaling factors (right) per pollutant, averaged for all sectors.

Figure 6 shows the spread in country-specific correlation lengths and scaling factors per pollutant, averaged over all sectors. The average correlation lengths are often larger than zero. This means that spatial correlations play an important role in ensuring that the gridded uncertainties don't cancel each other out at the country-level. Generally, the larger the country, the larger the correlation length needed. The median scaling factors are generally slightly above one, meaning that with the maximum correlation length the country-total uncertainty is not sufficiently high and the gridded uncertainties are upscaled. An exception is CO_2, which often shows scaling factors smaller than one. The reason is that the country-level uncertainties for CO_2 are small and summing up all gridded uncertainties leads to a larger combined uncertainty than what the countries report. Therefore, gridded uncertainties are downscaled and correlation lengths are often zero.

The largest correlation lengths appear for road transport, waste and other stationary combustion (Figure 7). For these sectors, the sum of the gridded uncertainties is too small to end up with the country-level emission uncertainty. This also results in occasional upscaling of the gridded emission uncertainties. In contrast, gridded uncertainties from the public power and industry sectors are often downscaled and receive low correlation lengths.

https://doi.org/10.5194/essd-2026-77
Preprint. Discussion started: 27 March 2026
© Author(s) 2026. CC BY 4.0 License.

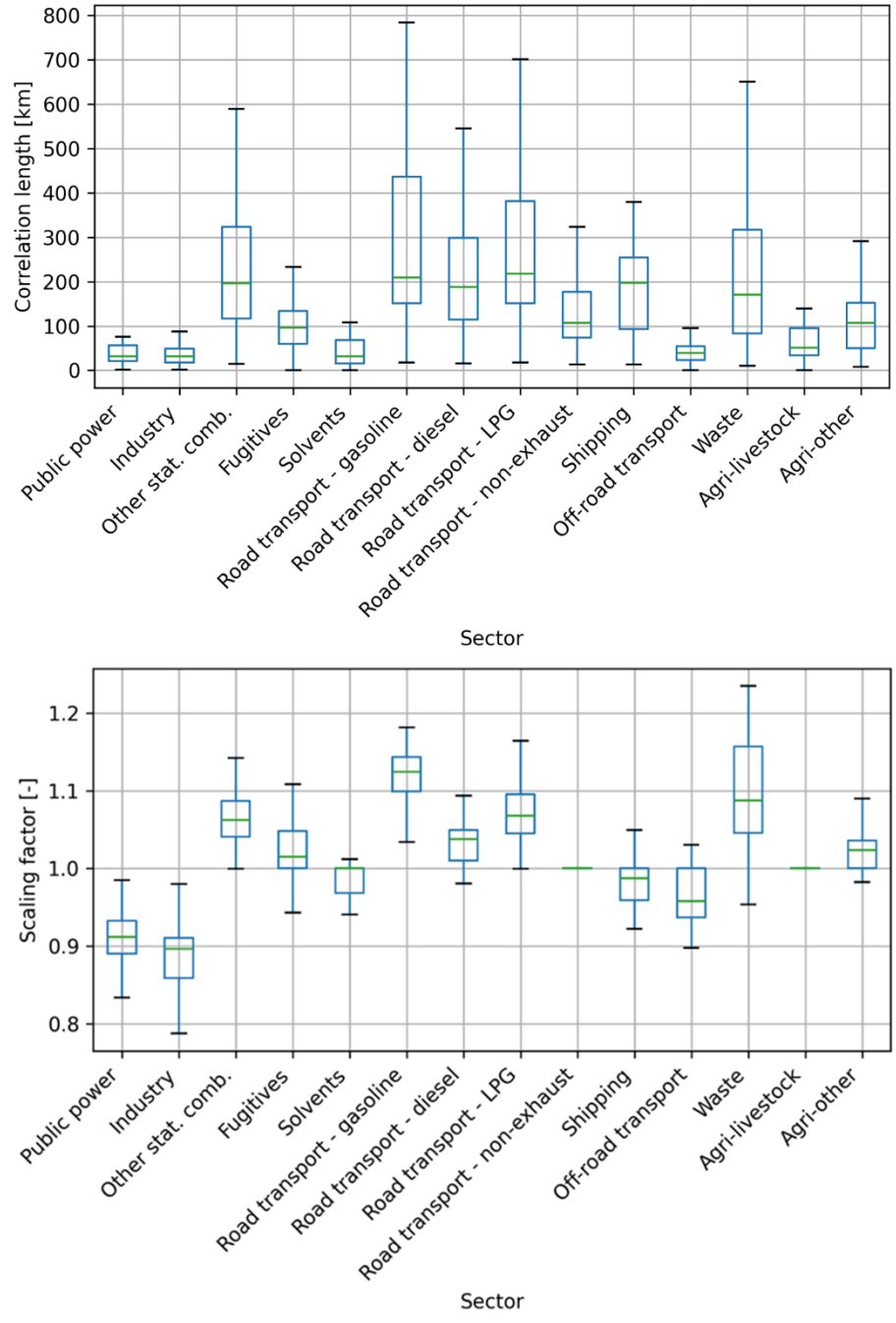

Figure 7: Box plot of country-specific correlation lengths (top) and scaling factors (bottom) per sector, averaged for all pollutants.

These results illustrate the importance of the optimization procedure. Without this step, the gridded and country-level emission uncertainties would be inconsistent. The optimized data, in combination with the spatial error correlation lengths, allow users to work with the data at any spatial resolution.

https://doi.org/10.5194/essd-2026-77
Preprint. Discussion started: 27 March 2026
© Author(s) 2026. CC BY 4.0 License.

4 Discussion

4.1 Comparison to other uncertainty estimates

The quantification of gridded emission uncertainties is a complex process and relies heavily on the inventory's source data and processing steps. We present an uncertainty estimate that propagates the uncertainties from the source data to the final product, following all the steps taken in the inventory preparation, ensuring consistency between the gridded emissions and their uncertainties. Previous efforts to estimate emission uncertainties have resulted in a wide range of uncertainty values. The number of studies looking quantitatively at gridded emission uncertainties is, however, limited. We discuss the most relevant scientific research below, starting with country-level/regional emission uncertainties, for which more studies are available. We list all uncertainties as relative standard deviation, unless indicated otherwise.

In this work, we use, where possible, reported country-level emission uncertainties at a detailed sector/fuel level. Most countries use a Monte Carlo simulation to calculate these uncertainties, and we consider them relatively reliable. Differences between countries occur mostly when the input data, such as the activity estimates, are more or less well-known. This is also expressed in the work by Choulga et al. (2021). They examined country-level CO_2 emission uncertainties on a global scale, where they separate between countries with a well-developed and a less well-developed statistical infrastructure. The first group, to which most of the countries in our domain belong, receives lower uncertainties. The average uncertainty for both groups is ~ 3.5 %. Our estimate of 1-2 % is in line with this. Moreover, Oda et al. (2019) estimate an uncertainty of 2.2 % in the total Polish CO_2 emissions, while Gurney et al. (2020) estimate an 8 % uncertainty in the total CO_2 emissions of the US based on their Vulcan emission inventory. In contrast, Kurokawa and Ohara (2020) estimate emission uncertainties over Asia that are much higher than our estimates (e.g., up to 13 % for CO_2 and up to 68 % for CO), mainly because they assume high uncertainties in activity data, which are unrealistic for European countries.

Most estimates of gridded emission uncertainties rely on a comparison of multiple inventories. Although this gives a hint on what the uncertainties could be, a point-by-point comparison of two datasets tends to give more extreme ranges, especially when including coarse, large-scale inventories in the comparison. For example, Gurney et al. (2020) compared two gridded CO_2 inventories for the US, resulting in a mean absolute relative difference (MARD) of 104.3 % at 1x1 km^2 resolution. Statistically, the relative standard deviation should be larger than the MARD, which suggests our gridded uncertainties are much lower (Table 3). Our spatial resolution is also lower, which could partly compensate for the difference. Using a similar approach, Oda et al. (2019) found systematic differences between two CO_2 emission inventories over Poland, with one inventory showing underestimations in urban areas (10-30 % bias). Overall, the gridded emission uncertainties range from 10 to 100 %, which is again higher than what we estimate. Finally, Andres et al. (2016) found an average gridded CO_2 emission uncertainty of 60 % globally, for an inventory at 1x1° resolution. This values falls between the uncertainty ranges for optimized and non-optimized countries and could therefore be fairly representative for the average of the whole domain.

Another way to validate the quality of the emission inventory is by comparing simulated atmospheric concentrations, using the emission inventory as model input, to observed concentrations. Since models and observations also induce uncertainties,

https://doi.org/10.5194/essd-2026-77
Preprint. Discussion started: 27 March 2026
© Author(s) 2026. CC BY 4.0 License.

we cannot fully attribute the differences to the emission inventory. Nevertheless, to provide an example, Oliviera et al. (2024) compared modelled and observed concentrations of different NMVOC compounds and found normalized mean biases of -24.6 % (toluene) to -71.2 % (xylene) in Spain. Our gridded NMVOC uncertainty range falls between those values.

As far as we are aware, the only study doing a detailed uncertainty analysis of gridded emission uncertainties if from Hogue et al. (2016), who end up with gridded uncertainties of around 160 % for CO_2 emissions over the US. This is much larger than what we calculated (Table 3), as the work of Hogue et al. is based on a gridded inventory using only population density for the spatial distribution of area source emissions, with introduces a large uncertainty.

Generally, we conclude that our gridded emission uncertainties are lower than what was found in previous studies. This is mainly due to the methodology applied in this work, which tends to dampen extreme values, unlike the point-by-point comparison of two datasets. Moreover, some of the previous studies have focused on emission inventories which are much less detailed than the CAMS-REG inventory, inherently causing uncertainties to be larger. Finally, we include a spatial error correlation length, which allows the gridded uncertainties to remain lower. We argue that the methodology applied in this work provides a more realistic estimate of the uncertainties in the emission inventory, considering all the input data and processing steps, making it a unique product. Also, note that previous studies have focused mostly on CO_2 and a quantitative evaluation of gridded air pollutant emission inventories is lacking all together. In this work, all pollutants are included in a consistent manner.

4.2 Study limitations and uncertainty in the uncertainties

The basis of our uncertainty propagation is formed by the reported, country-level emission uncertainties by Annex-I countries. Although the reported uncertainties are generally similar for all countries, we found some outliers for particular countries and sector/fuel combinations. Some of these were corrected after comparing them against other reporting years and checking with the reporting agencies, as these values turned out to be typos. However, this illustrates the need for manual checks, which will not necessarily capture all mistakes made in the reporting. This is one source of error we need to cope with, although the impact on the final product will be minor in most cases.

Moreover, the way we treat countries without detailed emission reporting leaves more room for errors. We apply average uncertainties based on the Annex-I countries, which are not representative for countries in Northern Africa or the Middle East in terms of emission landscape. Moreover, we do not consider the possibility that the non-Annex-I countries may have a weaker statistical infrastructure and therefore likely higher emission uncertainties, as suggested by Choulga et al. (2021). We partly compensate for this by adding a high grid-level uncertainty (100 % relative standard deviation), but the uncertainty on this estimate is large.

Also in other places we use expert judgement, for example, in estimating the uncertainty related to the representativeness of the proxy data. This introduces an additional uncertainty. When applying expert judgement the aim is to be conservative (i.e., on the high side), because the uncertainties need to be large enough to allow an inversion system enough degrees of freedom to get to the correct solution.

https://doi.org/10.5194/essd-2026-77
Preprint. Discussion started: 27 March 2026
© Author(s) 2026. CC BY 4.0 License.

In this work, we ignore error correlations between sectors and pollutants, which occur due to shared input data. For example, a particular proxy may be used for the spatial distribution of emissions from multiple sectors, but it is also applied to all pollutants. Additionally, all pollutants share their activity data. The impact of shared activity data on the error correlation between CO and CO_2 emissions has been analyzed in previous work (Super et al., 2024). Although these error correlations have proven useful in a multi-species inversion, we have so far been unable to incorporate these in the optimization procedure. Adding error correlations between sectors will likely increase the gridded uncertainties, but the exact impact cannot be quantified at this point.

4.3 Application in practice

The uncertainties product described in this paper is the result of several years of building up a process, step by step. Some intermediate results have been described in scientific papers (Super et al., 2020; Super et al., 2024) and these results have been tested in multiple projects and by different users (e.g., Scarpelli et al., 2024). This resulted in useful feedback, that helped us improve and extend our process and final product. For example, the work presented by Super et al. (2024) had separate gridded uncertainties and country-level uncertainties, that had to be combined by the user. We improved the user friendliness by providing only gridded uncertainties, which already incorporate the country-level uncertainties. By adding the optimization step the different estimates are now fully consistent, adding to the usability of this product.

We make use of a particular CAMS-REG version, in this case CAMS-REG v8.1 for 2022, and the uncertainties are consistent with the emissions in this inventory. We expect the uncertainties to be applicable to other recent CAMS-REG versions as well, as the reported uncertainties and emissions do not change drastically from one year to the next, unless some major event occurs (e.g., the COVID pandemic). However, over several years, emission trends become significant and users should be more careful using uncertainty estimates for older years. Moreover, since the presented emission uncertainties are based on a specific emission inventory, it does not necessarily represent uncertainties in European-scale emission inventories in general. The application to other regional inventories is therefore not advised.

5 Data availability

Gridded emission uncertainties (relative standard deviations) and spatial error correlation lengths (in degrees and kilometres) are available for all pollutants and sectors included in the CAMS-REG v8.1 emission inventory. The data are provided as NetCDF (Network Common Data Format) files at a resolution of 0.05 ° × 0.1 ° (latitude–longitude) for the European domain (30–72 ° N, 30 ° W–60 ° E): https://doi.org/10.5281/zenodo.18400810 (Super et al., 2026).

https://doi.org/10.5194/essd-2026-77
Preprint. Discussion started: 27 March 2026
© Author(s) 2026. CC BY 4.0 License.

Open Access Earth System Science Data Discussions

6 Conclusions and outlook

We present a detailed methodology to estimate uncertainties in the gridded CAMS-REG European emission inventory, starting from the most detailed input data and propagating all uncertainties to the final emission inventory. All pollutants are treated similarly, providing a consistent uncertainty estimate across all sector and pollutants.

We have previously illustrated the benefit of including error correlations between pollutants for multi-species inversions (Super et al., 2024). Although this is currently not included in the dataset, we will continue to work on this in the future. Similarly, temporal variations are not considered at this point, as they are not part of the CAMS-REG inventory. Nevertheless, the approach presented here could be applied to temporal profiles, adding an additional dimension.

Finally, the optimization procedure is currently done per country, which provides a spatial error correlation length per country, pollutant and sector. We are exploring options to combine the optimization parameters in a European map, making the uncertainties product more user-friendly.

Appendix A

Table A1: List of all regions included in the domain and the category they belong to. We separate between countries with detailed emission reporting, that are included in the optimization procedure ('Optimized'); countries without detailed emission reporting ('Non-optimized'); and sea regions.

Region name	Region category
Albania	Optimized
Algeria	Non-optimized
Armenia	Non-optimized
Atlantic Ocean	Sea region
Austria	Optimized
Azerbaijan	Non-optimized
Baltic Sea	Sea region
Barents Sea	Sea region
Belarus	Optimized
Belgium	Optimized
Black Sea	Sea region
Bosnia and Herzegovina	Optimized
Bulgaria	Optimized
Caspian Sea	Sea region
Croatia	Optimized
Cyprus	Optimized

https://doi.org/10.5194/essd-2026-77
Preprint. Discussion started: 27 March 2026
© Author(s) 2026. CC BY 4.0 License.

Czech Republic	Optimized
Denmark	Optimized
Egypt	Non-optimized
English Channel	Sea region
Estonia	Optimized
Finland	Optimized
France	Optimized
Georgia	Non-optimized
Germany	Optimized
Greece	Optimized
Greenland	Non-optimized
Greenland Sea	Sea region
Hungary	Optimized
Iceland	Optimized
Iran	Non-optimized
Iraq	Non-optimized
Ireland	Optimized
Irish Sea	Sea region
Israel	Non-optimized
Italy	Optimized
Jordan	Non-optimized
Kara Sea	Sea region
Kazakhstan	Non-optimized
Kosovo	Optimized
Kuwait	Non-optimized
Latvia	Optimized
Lebanon	Non-optimized
Libya	Non-optimized
Lithuania	Optimized
Luxembourg	Optimized
Malta	Optimized
Mediterranean Sea	Sea region
Moldova	Optimized

https://doi.org/10.5194/essd-2026-77
Preprint. Discussion started: 27 March 2026
© Author(s) 2026. CC BY 4.0 License.

Montenegro	Optimized
Morocco	Non-optimized
Netherlands	Optimized
North Macedonia	Optimized
North Sea	Sea region
Norway	Optimized
Norwegian Sea	Sea region
Poland	Optimized
Portugal	Optimized
Romania	Optimized
Russian Federation	Non-optimized
Saudi Arabia	Non-optimized
Serbia	Optimized
Slovakia	Optimized
Slovenia	Optimized
Spain	Optimized
Sweden	Optimized
Switzerland	Optimized
Syria	Non-optimized
Tunisia	Non-optimized
Turkey	Optimized
Turkmenistan	Non-optimized
Ukraine	Optimized
United Kingdom	Optimized
Uzbekistan	Non-optimized

Author contributions

IS collected the input data and developed/performed the error propagation, with input from JK. IS and BJ developed the model code for the error propagation. DM and AS developed the optimization procedure. IS prepared the manuscript with contributions from all co-authors.

https://doi.org/10.5194/essd-2026-77
Preprint. Discussion started: 27 March 2026
© Author(s) 2026. CC BY 4.0 License.

Open Access Earth System Science Data Discussions

Competing interests

The authors declare that they have no conflict of interest.

Acknowledgements

This research received funding from the European Union under grant agreement No 958927 (CoCO2), grant agreement No 101082194 (CORSO), and grant agreement No 101082125 (CAMEO).

References

Albarus, I., Fleischmann, G., Aigner, P., Ciais, P., Denier van der Gon, H., Dröge, R., Lian, J., Narvaez Rincon, M. A., Utard, H., and Lauvaux, T.: From political pledges to quantitative mapping of climate mitigation plans: Comparison of two European cities, Carbon Balance Manag., 18, 18, https://doi.org/10.1186/s13021-023-00236-y, 2023.

Andela, N., Kaiser, J. W., Heil, A., van Leeuwen, T. T., Wooster, M. J., van der Werf, G. R., Remy, S., and Schultz, M. G.: Assessment of the Global Fire Assimilation System (GFASv1), ECMWF, Reading, England, 2013.

Andres, R. J., Boden, T. A., and Higdon, D. M.: Gridded uncertainty in fossil fuel carbon dioxide emission maps, a CDIAC example, Atmos. Chem. Phys., 16, 14979–14995, https://doi.org/10.5194/acp-16-14979-2016, 2016.

Archila Bustos, M. F., Hall, O., Niedomysl, T., and Ernstson, U.: A pixel level evaluation of five multitemporal global gridded population datasets: a case study in Sweden, 1990–2015, Popul. Environ., 42, 255–277, https://doi.org/10.1007/s11111-020-00360-8, 2020.

Choulga, M., Janssens-Maenhout, G., Super, I., Solazzo, E., Agusti-Panareda, A., Balsamo, G., Bousserez, N., Crippa, M., Denier van der Gon, H., Engelen, R., Guizzardi, D., Kuenen, J., McNorton, J., Oreggioni, G., and Visschedijk, A.: Global anthropogenic CO2 emissions and uncertainties as a prior for Earth system modelling and data assimilation, Earth Syst. Sci. Data, 13, 5311–5335, https://doi.org/10.5194/essd-13-5311-2021, 2021.

Copernicus: CORINE Land Cover: https://land.copernicus.eu/en/products/corine-land-cover?tab=technical_summary, last access: 23 July 2024.

Crippa, M., Guizzardi, D., Muntean, M., Schaaf, E., Dentener, F., van Aardenne, J. A., Monni, S., Doering, U., Olivier, J. G. J., Pagliari, V., and Janssens-Maenhout, G.: Gridded emissions of air pollutants for the period 1970–2012 within EDGAR v4.3.2, Earth Syst. Sci. Data, 10, 1987–2013, https://doi.org/10.5194/essd-10-1987-2018, 2018.

Doumbia, T., Granier, C., Elguindi, N., Bouarar, I., Darras, S., Brasseur, G., Gaubert, B., Liu, Y., Shi, X., Stavrakou, T., Tilmes, S., Lacey, F., Deroubaix, A., and Wang, T.: Changes in global air pollutant emissions during the COVID-19 pandemic: a dataset for atmospheric modeling, Earth Syst. Sci. Data, 13, 4191–4206, https://doi.org/10.5194/essd-13-4191-2021, 2021.

https://doi.org/10.5194/essd-2026-77
Preprint. Discussion started: 27 March 2026
© Author(s) 2026. CC BY 4.0 License.

Eggleston H. S., Buendia L., Miwa K., Ngara T. and Tanabe, K. (Eds.): 2006 IPCC Guidelines for National Greenhouse Gas Inventories Prepared by the National Greenhouse Gas Inventories Programme, IGES, Hayama, Japan, ISBN 4-88788-032-4 , 2006.

EMEP: Data reported by Parties under LRTAP Convention: https://www.ceip.at/webdab-emission-database/officially-reported-activity-data, last access: 1 August 2023.

European Commission: Joint Research Centre, Atmospheric monitoring and inverse modelling for verification of greenhouse gas inventories, Publications Office, https://data.europa.eu/doi/10.2760/759928, 2018.

European Environment Agency: EMEP/EEA air pollutant emission inventory guidebook 2019: Technical guidance to prepare national emission inventories, European Environment Agency, Copenhagen, Denmark, 2019.

Gao, W., Balmer, M., and Miller, E. J.: Comparison of MATSim and EMME/2 on Greater Toronto and Hamilton Area Network, Canada, Transp. Res. Rec., 2197, 118–128, https://doi.org/10.3141/2197-14, 2010.

Gately, C. K. and Hutyra, L. R.: Large uncertainties in urban-scale carbon emissions, J. Geophys. Res. Atmos., 122, 242–260, https://doi.org/https://doi.org/10.1002/2017JD027359, 2017.

German, R., Matthews, B., and Ruyssenaars, P.: Inverse modelling as a tool to support national greenhouse gas monitoring in Europe, European Topic Centre on Climate change mitigation and energy, Mol, Belgium, Eionet Report - ETC/CME 4/2021, 2021.

Grigoriadis, A., Mamarikas, S., Ioannidis, I., Majamäki, E., Jalkanen, J.-P., and Ntziachristos, L.: Development of exhaust emission factors for vessels: A review and meta-analysis of available data, Atmos. Environ.: X, 12, 100142, https://doi.org/https://doi.org/10.1016/j.aeaoa.2021.100142, 2021.

Grythe, H., Lopez-Aparicio, S., Vogt, M., Vo Thanh, D., Hak, C., Halse, A. K., Hamer, P., and Santos, G. S.: The MetVed model: development and evaluation of emissions from residential wood combustion at high spatio-temporal resolution in Norway, Atmos. Chem. Phys., 19, 10217–10237, https://doi.org/10.5194/acp-19-10217-2019, 2019.

Gurney, K. R., Liang, J., Patarasuk, R., Song, Y., Huang, J., and Roest, G.: The Vulcan Version 3.0 High-Resolution Fossil Fuel CO2 Emissions for the United States, J. Geophys. Res.-Atmos., 125, 19, https://doi.org/10.1029/2020JD032974, 2020.

Hogue, S., Marland, E., Andres, R. J., Marland, G., and Woodard, D.: Uncertainty in gridded CO2 emissions estimates, Earth's Futur., 4, 225–239, https://doi.org/10.1002/2015EF000343, 2016.

Hutchins, M. G., Colby, J. D., Marland, G., and Marland, E.: A comparison of five high-resolution spatially-explicit, fossil-fuel, carbon dioxide emission inventories for the United States, Mitig. Adapt. Strat. Gl., 22, 947–972, https://doi.org/https://doi.org/10.1007/s11027-016-9709-9, 2017.

Jalkanen, J.-P., Johansson, L., Kukkonen, J., Brink, A., Kalli, J., and Stipa, T.: Extension of an assessment model of ship traffic exhaust emissions for particulate matter and carbon monoxide, Atmos. Chem. Phys., 12, 2641–2659, https://doi.org/10.5194/acp-12-2641-2012, 2012.

Johansson, L., Jalkanen, J.-P., and Kukkonen, J.: Global assessment of shipping emissions in 2015 on a high spatial and temporal resolution, Atmos. Environ., 167, 403–415, https://doi.org/https://doi.org/10.1016/j.atmosenv.2017.08.042, 2017.

https://doi.org/10.5194/essd-2026-77
Preprint. Discussion started: 27 March 2026
© Author(s) 2026. CC BY 4.0 License.

Keita, S., Liousse, C., Assamoi, E.-M., Doumbia, T., N'Datchoh, E. T., Gnamien, S., Elguindi, N., Granier, C., and Yoboué, V.: African Anthropogenic Emissions Inventory for Gases and Particles from 1990 to 2015, Earth Syst. Sci. Data, 13, 3691–3705, https://doi.org/10.5194/essd-13-3691-2021, 2021.

Kuenen, J., Dellaert, S., Visschedijk, A., Jalkanen, J.-P., Super, I., and Denier Van Der Gon, H.: CAMS-REG-v4: a state-of-the-art high-resolution European emission inventory for air quality modelling, Earth Syst. Sci. Data, 14, 491–515, https://doi.org/10.5194/essd-14-491-2022, 2022.

Kuipers, J. B.: Quaternions and Rotation Sequences: A Primer with Applications to Orbits, Aerospace, and Virtual Reality, Princeton University Press, Princeton, NJ, 371 pp., ISBN 9780691102986, 1999.

Kunik, L., Mallia, D. V., Gurney, K. R., Mendoza, D. L., Oda, T., and Lin, J. C.: Bayesian inverse estimation of urban CO2 emissions: Results from a synthetic data simulation over Salt Lake City, UT, Elem. Sci. Anth., 7, 36, https://doi.org/https://doi.org/10.1525/elementa.375, 2019.

Kurokawa, J. and Ohara, T.: Long-Term Historical Trends in Air Pollutant Emissions in Asia: Regional Emission Inventory in ASia (REAS) Version 3, Atmos. Chem. Phys., 20, 12761–12793, https://doi.org/10.5194/acp-20-12761-2020, 2020.

Lauvaux, T., Miles, N. L., Deng, A., Richardson, S. J., Cambaliza, M. O., Davis, K. J., Gaudet, B., Gurney, K. R., Huang, J., O'Keefe, D., Song, Y., Karion, A., Oda, T., Patarasuk, R., Razlivanov, I., Sarmiento, D., Shepson, P., Sweeney, C., Turnbull, J., and Wu, K.: High-resolution atmospheric inversion of urban CO2 emissions during the dormant season of the Indianapolis Flux Experiment (INFLUX), J. Geophys. Res.-Atmos., 121, 5213–5236, https://doi.org/10.1002/2015JD024473, 2016.

Lorente, A., Boersma, K. F., Eskes, H. J., Veefkind, J. P., van Geffen, J. H. G. M., de Zeeuw, M. B., Denier van der Gon, H. A. C., Beirle, S., and Krol, M. C.: Quantification of nitrogen oxides emissions from build-up of pollution over Paris with TROPOMI, Sci. Rep., 9, 20033, https://doi.org/10.1038/s41598-019-56428-5, 2019.

McDuffie, E. E., Smith, S. J., O'Rourke, P., Tibrewal, K., Venkataraman, C., Marais, E. A., Zheng, B., Crippa, M., Brauer, M., and Martin, R. V.: A global anthropogenic emission inventory of atmospheric pollutants from sector- and fuel-specific sources (1970–2017): an application of the Community Emissions Data System (CEDS), Earth Syst. Sci. Data, 12, 3413–3442, https://doi.org/10.5194/essd-12-3413-2020, 2020.

Musollari, S., Pseftogkas, A., Koukouli, M.-E., Manders, A., Segers, A., Garane, K., and Balis, D.: The Spatiotemporal Variability of Ozone and Nitrogen Dioxide in the Po Valley Using In Situ Measurements and Model Simulations, Remote Sens., 17, 1794, https://doi.org/10.3390/rs17101794, 2025.

Oda, T., Bun, R., Kinakh, V., Topylko, P., Halushchak, M., Marland, G., Lauvaux, T., Jonas, M., Maksyutov, S., Nahorski, Z., Lesiv, M., Danylo, O., and Joanna, H.-P.: Errors and uncertainties in a gridded carbon dioxide emissions inventory, Mitig. Adapt. Strateg. Glob. Change, 24, 1007–1050, https://doi.org/10.1007/s11027-019-09877-2, 2019.

Oliveira, K., Guevara, M., Jorba, O., Petetin, H., Bowdalo, D., Tena, C., Montané Pinto, G., López, F., and Pérez García-Pando, C.: On the uncertainty of anthropogenic aromatic volatile organic compound emissions: model evaluation and sensitivity analysis, Atmos. Chem. Phys., 24, 7137–7177, https://doi.org/10.5194/acp-24-7137-2024, 2024.

https://doi.org/10.5194/essd-2026-77
Preprint. Discussion started: 27 March 2026
© Author(s) 2026. CC BY 4.0 License.

Pillai, D., Buchwitz, M., Gerbig, C., Koch, T., Reuter, M., Bovensmann, H., Marshall, J., and Burrows, J. P.: Tracking city CO2 emissions from space using a high-resolution inverse modelling approach: a case study for Berlin, Germany, Atmos. Chem. Phys., 16, 9591–9610, https://doi.org/10.5194/acp-16- 9591-2016, 2016.

Press, W. H., Teukolsky, S. A., Vetterling, W. T., and Flannery, B. P.: Numerical Recipes in C (2nd ed.): The Art of Scientific Computing, Cambridge University Press, New York, NY, 1992.

Raney, B., Cetin, N., Völlmy, A., Vrtic, M., Axhausen, K., and Nagel, K.: An agent-based microsimulation model of Swiss travel: First results, Networks Spat. Econ., 3, 23–41, https://doi.org/10.1023/A:1022096916806, 2003.

Robinson, T. P., Wint, G. R. W., Conchedda, G., Van Boeckel, T. P., Ercoli, V., Palamara, E., Cinardi, G., D'Aietti, L., Hay, S. I., and Gilbert, M.: Mapping the Global Distribution of Livestock, PLoS ONE, 9, e96084, https://doi.org/10.1371/journal.pone.0096084, 2014.

Scarpelli, T. R., Palmer, P. I., Lunt, M., Super, I., and Droste, A.: Verifying national inventory-based combustion emissions of CO2 across the UK and mainland Europe using satellite observations of atmospheric CO and CO2, Atmos. Chem. Phys., 24, 10773–10791, https://doi.org/10.5194/acp-24-10773-2024, 2024.

Siouti, E., Skyllakou, K., Patoulias, D., Athanasopoulou, E., Mihalopoulos, N., Kuenen, J., and Pandis, S.N.: High resolution source-resolved PM2.5 spatial distribution and human exposure in a large urban area, Atmos. Environ., 355, 121277, https://doi.org/10.1016/j.atmosenv.2025.121277, 2025.

Super, I., Dellaert, S. N. C., Visschedijk, A. J. H., and Van Der Gon, H. A. C. D.: Uncertainty analysis of a European high-resolution emission inventory of CO2 and CO to support inverse modelling and network design, Atmos. Chem. Phys., 20, 1795–1816, https://doi.org/https://doi.org/10.5194/acp-20-1795-2020, 2020.

Super, I., Scarpelli, T., Droste, A., and Palmer, P. I.: Improved definition of prior uncertainties in CO2 and CO fossil fuel fluxes and its impact on multi-species inversion with GEOS-Chem (v12.5), Geosci. Model Dev., 17, 7263–7284, https://doi.org/10.5194/gmd-17-7263-2024, 2024.

Super, I., Mathas, D., Jonkheid, B., Segers, A., and Kuenen, K.: CAMS-REG-UNC-v8.1: A detailed uncertainty product for the gridded CAMS-REG-v8.1 emission inventory (1.0), Zenodo [data set], https://doi.org/10.5281/zenodo.18400810, 2026.

Tenkanen, M. K., Tsuruta, A., Tyystjärvi, V., Törmä, M., Autio, I., Haakana, M., Tuomainen, T., Leppänen, A., Markkanen, T., Raivonen, M., Niinistö, S., Arslan, A. N., and Aalto, T.: Using Atmospheric Inverse Modelling of Methane Budgets with Copernicus Land Water and Wetness Data to Detect Land Use-Related Emissions, Remote Sens., 16, 124, https://doi.org/10.3390/rs16010124, 2024.

Tokaya, J. P., Kranenburg, R., Timmermans, R. M. A., Coenen, P. W. H. G., Kelly, B., Hullegie, J. S., Megaritis, T., and Valastro, G.: The impact of shipping on the air quality in European port cities with a detailed analysis for Rotterdam, Atmos. Environ.: X, 23, 100278, https://doi.org/10.1016/j.aeaoa.2024.100278, 2024.

UNFCCC: National Inventory Submissions 2020: https://unfccc.int/ghg-inventories-annex-i-parties/2020, last access: 31 January 2024.

https://doi.org/10.5194/essd-2026-77
Preprint. Discussion started: 27 March 2026
© Author(s) 2026. CC BY 4.0 License.

Van Brummelen, G.: Heavenly Mathematics: The Forgotten Art of Spherical Trigonometry, Princeton University Press, Princeton, NJ, 216 pp., ISBN 9780691175997, 2017.

Van der A, R. J., Ding, J., and Eskes, H.: Monitoring European anthropogenic NOx emissions from space, Atmos. Chem. Phys., 24, 7523–7534, https://doi.org/10.5194/acp-24-7523-2024, 2024.

Wang, Z., Couvidat, F., and Sartelet, K.: Response of biogenic secondary organic aerosol formation to anthropogenic NOx emission mitigation, Sci. Total Environ., 927, 172142, https://doi.org/10.1016/j.scitotenv.2024.172142, 2024.